

Research Article

Investigation and Simulation of Mechanics of Solid Beam versus Sandwich Beams with Different Core Material

¹Mohamed A.M. Shehata, ¹Ahmed S.A. Abou-Taleb and ²Ahmed Nassef

¹Mechanical Engineering Department, Faculty of Engineering, Fayoum University, Egypt

²Production Engineering and Mechanical Design Department, Faculty of Engineering, Port-Said University, Egypt

Abstract: A solid steel beam versus sandwich beams with varied core material between polyamide, epoxy and wood was simulated numerically and analyzed theoretically to realize the difference between their mechanics. On the other hand, the length 300 mm, width 20 mm, total thickness 16 mm, face thickness 3 mm, core thickness 10 mm and steel faces material were kept constant. The concerned mechanics were under a bending moment, an axial load and a combination of both loadings. The results indicate that the different stresses types of bending stress, normal stress and these two stresses combined can be significantly varied due to a change in the flexural rigidity and the transformation factor, which can be done via utilization sandwich beam advantages over a solid beam having the same dimensions. Also, with a lower variance degree, the change in stresses values can be done by using sandwich beams with a contrastive core material.

Keywords: Bending stress, combined loadings, flexural rigidity, normal stress, sandwich beam, transformation factor

INTRODUCTION

The most important advantages of the sandwich beam structures are high strength to weight ratio, high bending resistance and buckling resistance and good flexibility. These advantages offer the designers a crucial specifications to be implemented in various demanded applications such as mechanical engineering, sustainable-energy, aerospace and civil fields, where weight saving has been, as always, a major design factor for more than 50 years as mentioned in Kim and Sawanson (2001), Magnucka-Blandzi and Magnucki (2007) and Bozhevolnaya *et al.* (2008).

The sandwich beam components are simply assembly layers, where two thin but stiff and strong face sheets bonded to a thick but light-weight core by an adhesive material. The faces carry bending stresses, while the core keeps the faces in positions from each other and resists torsion and transverse shear forces. Therefore these sandwich beam structures can carry loads, maintaining high strength and stiffness to weight parameters and exhibit good stability under compression as stated by Chen *et al.* (2001).

The analysis of sandwich beams mechanics strongly depends on some main parameters or

assumptions, where the three layers of the sandwich beam are homogeneous, isotropic and elastic, but at the same time rigidly joined together. Further, the upper and lower layers (faces) must be strong, stiff and thin; plus separated and bonded to a weaker, light and thick core. The sandwich beam must act as one whole specimen; therefore the adhesion of both materials is essential for the load transfer. The primary materials for producing strong faces are steel and aluminum, whereas the primary materials for the relatively soft core (middle layer) are rubber and honeycomb structures, these materials combinations for manufacturing sandwich beam are necessary to get the best of its advantages such as good bending stiffness besides good damping capacity as investigated by Banerjee *et al.* (2007).

An immense variance of core geometries is heavy implemented nowadays in daily applications around us. The most famous ones widely used are corrugated cores, honeycomb and foam. The honeycomb cores can be made from one material such as aluminum or composite materials as glass thermoplastic. If the application requirements need high thermal tolerance, the best choice will be the expanded foams. To achieve good bonding between sandwich beam components,

Corresponding Author: Mohamed A.M. Shehata, Mechanical Engineering Department, Faculty of Engineering, Fayoum University, Egypt, Tel.: +20 1004565665, +20 842150485

This work is licensed under a Creative Commons Attribution 4.0 International License (URL: <http://creativecommons.org/licenses/by/4.0/>).

usually, two types of adhesive bonding are commonly used for example co-curing and secondary bonding. An investigation was carried out to study the effect of the face sheet thickness on the fatigue strength of different types of sandwich beam specimens with aluminum honeycomb; it was concluded that there is no apparent relationship between them via Jen and Chang (2009).

Static analysis of sandwich beams was studied with taken into consideration the important effect of the scale of a basic cell. Classic beam, homogenization and finite element methods were carried out systematically to study typical cell configurations by Dai and Zhang (2008). It is concluded that, when the basic cell has a considerable dimension relative to the structural size, its effect is important; on the other hand this effect decreases rapidly with the basic cell size reduction.

For web-core sandwich beams, a stress analysis method was suggested; which depends on that the beam is a transverse cut from a sandwich plate. The main idea of this stress analysis method is transforming this complex configuration into a homogenous sandwich beam, where this substitute homogenous specimen is an equivalent for the initially periodic web-core sandwich beam constructed from a set of unit cells. Now, by analysis this homogenized beam follows thick face-plate kinematics, we can get the bending moment, deflection and shear force distributions. And then, the accurate calculations of the normal stress components can be obtained by reconsidering the periodic structure of the beam. The validation of this suggested analysis method is checked out with finite elements analyses via Romanoff *et al.* (2007).

Symmetric isotropic layers of a sandwich beam with a de-bond crack at the interface of core and face sheet are investigated utilizing a semi-analytic method, the two main basics of this method are linear elastic fracture mechanics and two-dimensional elasticity. The goal of this investigation is to study the effects of shear on energy release rate and the mix of mode fixity. Bending moments and axial forces were subjected to the sandwich beams to achieve solutions for a large variety of geometrical and material properties and overall loading conditions. The energy release rate which depends on the shear forces is explained from points of physical and mechanical views via utilizing structural mechanics concepts. Also, Barbieri *et al.* (2018) define the leading causes and effects of the near-tip deformations by introducing crack tip root rotations to account.

The behavior of sandwich beams components including both core and face sheets, which are made of green materials, are studied through experimental work. Three core configurations as three flute varieties in the form of corrugated cardboards were made and classified as B, C and BC flutes with bulk densities of 170, 127 and 138 kg/m³ respectively, whereas a Fiber-Reinforced Polymer (FRP) face sheets were made from a unidirectional flax fabric and a partial bio-based

epoxy. McCracken and Sadeghian (2018a) recommended for sandwich applications that required the highest strength and stiffness; the C flute is the best choice where it has the lowest bulk density and the highest availability in the market amongst all the three flutes. For building applications that need large-scale structural sandwich panels, we use the flax FRP skins combined with the corrugated cardboard cores as a green option for fabrication.

The relative performances of sandwich beams with various combinations of non-traditional pairs of materials were compared with each other by a systematic procedure in three-point bending. Steeves and Fleck (2004) stated that the new structures in the industry such as sandwich beams with foam or honeycomb cores are better from the point of view of bending stiffness to weight ratio, but the need for simple methods describing the mechanics of these complex structures is rising.

Four-point bending test was loaded up to failure, where total 30 small scale sandwich beam specimens were used. The samples were manufactured through six different beam varieties with dimensions of 50 mm width and 200 or 350 mm length. The neutral line position, curvature due to moment, strain and deflection were analyzed. The most important parameters to be calculated from the test results are core shear modulus, flexural rigidity and shear rigidity. Based on the geometry and material properties of sandwich beams, the model is prepared to quantify the degree of composite action. As a result due to a function of the relative stiffness of the face sheets and the core plus the length of the shear span, generally, the sandwich beams showed a partial composite behavior ranging from 15% to 91% of full one. McCracken and Sadeghian (2018b) concluded that the key factor in optimizing sandwich panels made of the core is the matching degree between the mechanical properties of the face sheet and core.

Sandwich beams face sheets are stiff and have high ability to absorb energy when exposed to shock loading through high plastic deformation, while cellular cores have different types such as honeycomb, foam or lattice as stated via Lu and Yu (2003), Gibson and Ashby (1997) and Ashby *et al.* (2000). For previous qualities, they are heavily used in applications need impact protection. Therefore the properties of sandwich beams such as impact absorption, failure mechanisms and deformation modes must be studied. Through our investigations, Xue and Hutchinson (2004), Fleck and Deshpande (2004) and McShane *et al.* (2007) concluded that metallic sandwich beams have higher blast resistance than monolithic structures with equal mass, because of core compression nature through plastic energy dissipation and the interaction effects as fluid-structure.

The main advantage of the Layered Sandwich Beam (LSB) is increasing sectional stability via protecting the composite faces from wrinkling,

buckling and indentation failure as mentioned by Ferdous *et al.* (2018). In the vertical orientation, the LSB improved its bending and shear strengths by 25% and 100%, respectively, according to single sandwich beams with the same orientation. The LSB fundamental behavior in vertical or horizontal orientations and different loading configurations can be reliably predicted by the simulation analysis using the finite element model, within a small difference in results.

The primary objective of this paper is to study the varied types of stresses occurred to sandwich beams with a different core material and a solid beam when subjected to various types of loadings as bending moment, axial load and combination of these loadings. Verifications of simulation results with theoretical calculations carried out by the present authors to select a suitable sandwich beam as a good substitute to a solid beam in different applications; due to the main advantages of sandwich beams, where the targeted one here is high stiffness to weight ratio.

THEORETICAL ANALYSIS

This analysis provides a discussion and a brief derivation about the equations needed for obtaining the theoretical results, where the main interest is about the comparison of mechanics between solid beam versus sandwich beam (Fig. 1) under different types of loads.

The targeted theoretical results are going to be centered on the flexural rigidity D and the transformation factor n , which will be the necessary parameters for determinations various types and combinations of stresses of the sandwich beams with a different core material. Where it is assumed that the materials are homogenous and isotropic, behave in a linear-elastic manner and no delamination or slipping occurred between the layers.

Flexural rigidity of the sandwich beam: Because of the flexural rigidity key importance for the theoretical calculations, the next section will introduce brief derivation steps of the flexural rigidity of symmetrical or unsymmetrical sandwich beam structure.

Bending stress diagram: The first step of this derivation is the bending stress diagram, as a consequence of applying a bending moment about an axis perpendicular to the specimen's axis of cross-section as shown in Fig. 2.

The resultant bending stress of an unsymmetrical sandwich beam, within cantilever geometry affected by the same previous bending moment, is drawn in Fig. 3.

From this Fig. 3, it can be easy measured the coordinates in the thickness direction (y_0, y_1, y_2 and y_3) of a sandwich beam, as mentioned in Eq. (1):

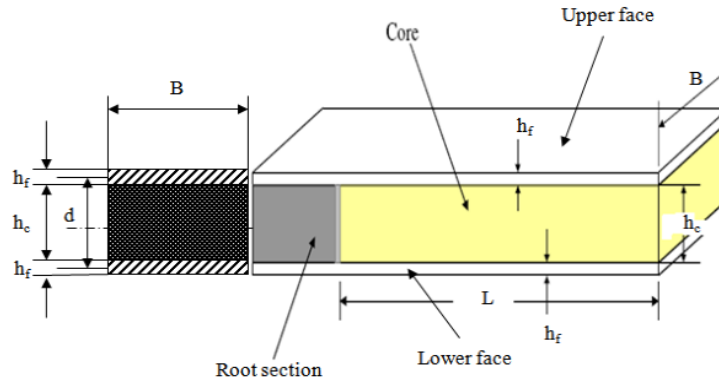


Fig. 1: Components, dimensions and cross-sectional area of a sandwich beam structure

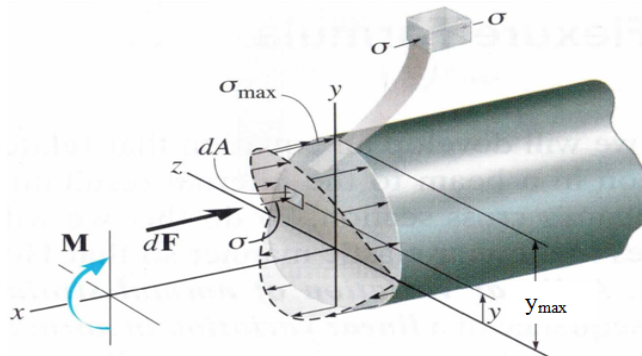


Fig. 2: Bending stress diagram of a normal specimen, not a sandwich one

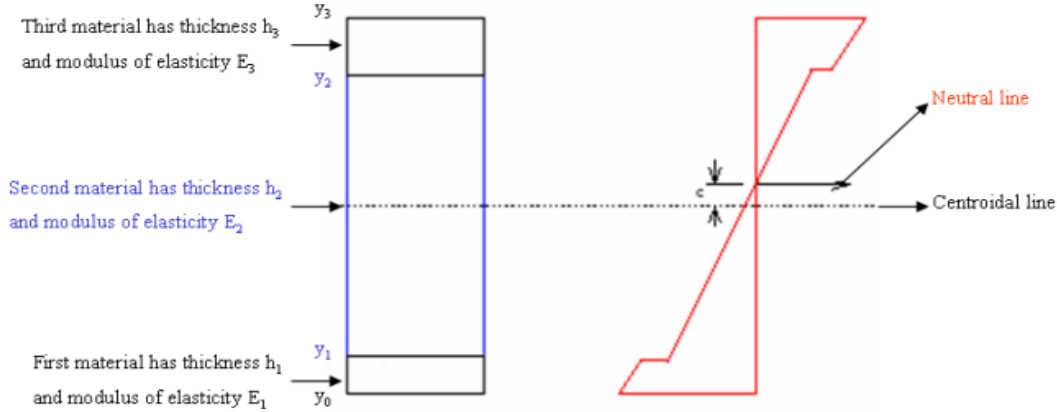


Fig. 3: Bending stress variation of an unsymmetrical sandwich beam

$$y_0 = c - \left(\frac{h_2}{2}\right) - h_1, y_1 = c - \left(\frac{h_2}{2}\right), y_2 = c + \left(\frac{h_2}{2}\right), \quad (1)$$

$$\text{and } y_3 = c + \left(\frac{h_2}{2}\right) + h_3$$

Neutral line offset: The second step is the calculations of the neutral line offset c from the centroidal line in Fig. 3, which based on the summation of forces as listed as follow:

$$\Sigma F = \int dF = \int \sigma dA = \int \sigma B dy = \int \frac{E_i y}{R} B dy,$$

$$\Sigma F = \left(\frac{B}{R}\right) \int E_i y dy = \text{Zero}.$$

By calculating the integration; the following expression can be obtained:

$$\left(\frac{B}{R}\right) * \left[\int_{y_0}^{y_1} E_1 y dy + \int_{y_1}^{y_2} E_2 y dy + \int_{y_2}^{y_3} E_3 y dy \right] = \text{Zero},$$

$$\left(\frac{B}{R}\right) * \left[\frac{1}{2} E_1 (y_1^2 - y_0^2) + \frac{1}{2} E_2 (y_2^2 - y_1^2) + \frac{1}{2} E_3 (y_3^2 - y_2^2) \right] = \text{Zero}.$$

Then by substitute the coordinates (y_0, y_1, y_2 and y_3) with their definitions from Eq. (1) and put the neutral line offset c term in the left-hand side, Eq. (2) can be obtained:

$$c = \frac{E_1 h_1 (h_1 + h_2) - E_3 h_3 (h_3 + h_2)}{2(E_1 h_1 + E_2 h_2 + E_3 h_3)} \quad (2)$$

$$= \frac{E_1 h_1 \left(\frac{h_1 + h_2}{2}\right) - E_3 h_3 \left(\frac{h_3 + h_2}{2}\right)}{(E_1 h_1 + E_2 h_2 + E_3 h_3)}$$

Therefore, Eq. (2) can be used to calculate the neutral line offset c from the centroidal line for different three-layered sandwich beams that have a

symmetrical or unsymmetrical cross-sectional area, which will be used further in this derivation.

Bending moment: The third step is the calculations of bending moment M_b of the cantilever sandwich beam when subjected to a similar moment as Fig. 2; therefore the calculations can be listed as follow:

$$M_b = \int y dF = \int y \sigma dA = \int y \sigma B dy,$$

$$M_b = \int y \frac{E_i y}{R} B dy = \left(\frac{B}{R}\right) \int E_i y^2 dy.$$

By calculating the integration; the following expression can be obtained:

$$M_b = \left(\frac{B}{R}\right) * \left[\int_{y_0}^{y_1} E_1 y^2 dy + \int_{y_1}^{y_2} E_2 y^2 dy + \int_{y_2}^{y_3} E_3 y^2 dy \right],$$

$$M_b = \left(\frac{B}{R}\right) * \left[\frac{1}{3} E_1 (y_1^3 - y_0^3) + \frac{1}{3} E_2 (y_2^3 - y_1^3) + \frac{1}{3} E_3 (y_3^3 - y_2^3) \right].$$

Then by substitute the coordinates (y_0, y_1, y_2 and y_3) with their definitions from Eq. (1) and put the bending moment M_b term in the left-hand side, Eq. (3) can be obtained:

$$M_b = \left(\frac{B}{R}\right) * \left\{ \frac{E_1}{3} \left[\left(c - \frac{h_2}{2}\right)^3 - \left(c - \frac{h_2}{2} - h_1\right)^3 \right] + E_2 c^2 h_2 + \frac{E_2 h_2^3}{12} + \frac{E_3}{3} \left[\left(c + \frac{h_2}{2} + h_3\right)^3 - \left(c + \frac{h_2}{2}\right)^3 \right] \right\} \quad (3)$$

Final equation of flexural rigidity of the sandwich beam: Since $\sigma = E_{eq} * (y/R) = (M_b * y)/I$, now the flexural rigidity D of the unsymmetrical sandwich beam structure can be derived in Eq. (4) as written below:

$$D = E_{eq} * I = M_b * R$$

$$= B * \left\{ \begin{aligned} & \frac{E_1}{3} \left[\left(c - \frac{h_2}{2} \right)^3 - \left(c - \frac{h_2}{2} - h_1 \right)^3 \right] + E_2 c^2 h_2 + \frac{E_2 h_2^3}{12} \\ & + \frac{E_3}{3} \left[\left(c + \frac{h_2}{2} + h_3 \right)^3 - \left(c + \frac{h_2}{2} \right)^3 \right] \end{aligned} \right\} \quad (4)$$

Bending stress of symmetric sandwich beam: To simplify obtaining the flexural rigidity D of symmetric sandwich beam composed of three layers as shown in Fig. 1, the following conditions ($c = 0$, $E_1 = E_3 = E_f$, $E_2 = E_c$, $h_1 = h_3 = h_f$ and $h_2 = h_c$) will be used. Also via considering d as the distance between the neutral lines of the two face sheets ($d = h_f + h_c$) in the previous Eq. (4), the output-come of flexural rigidity will be in Eq. (5) as follows:

$$D = B * \int E_y y^2 dy$$

$$= B * \left[\int_{-\frac{h_f}{2}}^{\frac{h_f}{2}} E_f y^2 dy + \int_{-\frac{h_c}{2}}^{\frac{h_c}{2}} E_c y^2 dy + \int_{\frac{h_f}{2}}^{\frac{h_f}{2} + \frac{h_c}{2}} E_f y^2 dy \right] \quad (5)$$

$$= (2B) * \left[\int_{\frac{h_f}{2}}^{\frac{h_f}{2} + \frac{h_c}{2}} E_f y^2 dy + \int_0^{\frac{h_c}{2}} E_c y^2 dy \right]$$

$$= B * \left[\frac{E_f h_f^3}{6} + \frac{E_f h_f d^2}{2} + \frac{E_c h_c^3}{12} \right]$$

$$= 2D_f + D_c + D$$

Therefore, the bending stresses and strains in the three layers of a sandwich beam structure can be written in Eq. (6) as follow:

$$\sigma_{Bf} = \frac{ME_f y}{D}, \text{ where: } \frac{h_c}{2} < |y| \leq \frac{h_c}{2} + h_f, \text{ also: } \varepsilon_{Bf} = \frac{\sigma_{Bf}}{E_f},$$

$$\sigma_{Bc} = \frac{ME_c y}{D}, \text{ where: } |y| \leq \frac{h_c}{2}, \text{ also: } \varepsilon_{Bc} = \frac{\sigma_{Bc}}{E_c}. \quad (6)$$

Axial load stress of sandwich beam: The stress of axially loaded sandwich beam can be obtained via deploying the transformation factor n . This dimensionless number n is a ratio between the moduli of elasticity of the two constructed face sheet and core materials of the sandwich beam. The purpose of using this factor n is transforming the sandwich beam from a composite beam to a single material beam. Therefore with the utilization of previous sandwich beam dimensions in Fig. 1; the stresses, strains and extension due to axial load for symmetric sandwich beam consists of three layers can be simplified in Eq. (7) as follow:

$$\sigma_{Nf} = \frac{F}{A} = \frac{F}{B * \left[2h_f + \left(\frac{E_c}{E_f} \right) * h_c \right]} = \frac{F}{B * [2h_f + n * h_c]}, \text{ also: } \sigma_{Nc} = n * \sigma_{Nf}.$$

$$\varepsilon_{Nf} = \frac{\sigma_{Nf}}{E_f} = \varepsilon_{Nc} = \frac{\sigma_{Nc}}{E_c}, \text{ also: } \Delta L = \frac{\sigma_{Nf}}{E_f} * L_o = \frac{\sigma_{Nc}}{E_c} * L_o. \quad (7)$$

Mass of sandwich beam: The primary objective of using sandwich beam structure is utilization its main advantage, which is high strength and stiffness to weight ratio; therefore the total mass of sandwich beam components is a necessary design factor to comprehend, as from Fig. 1; we can express Eq. (8):

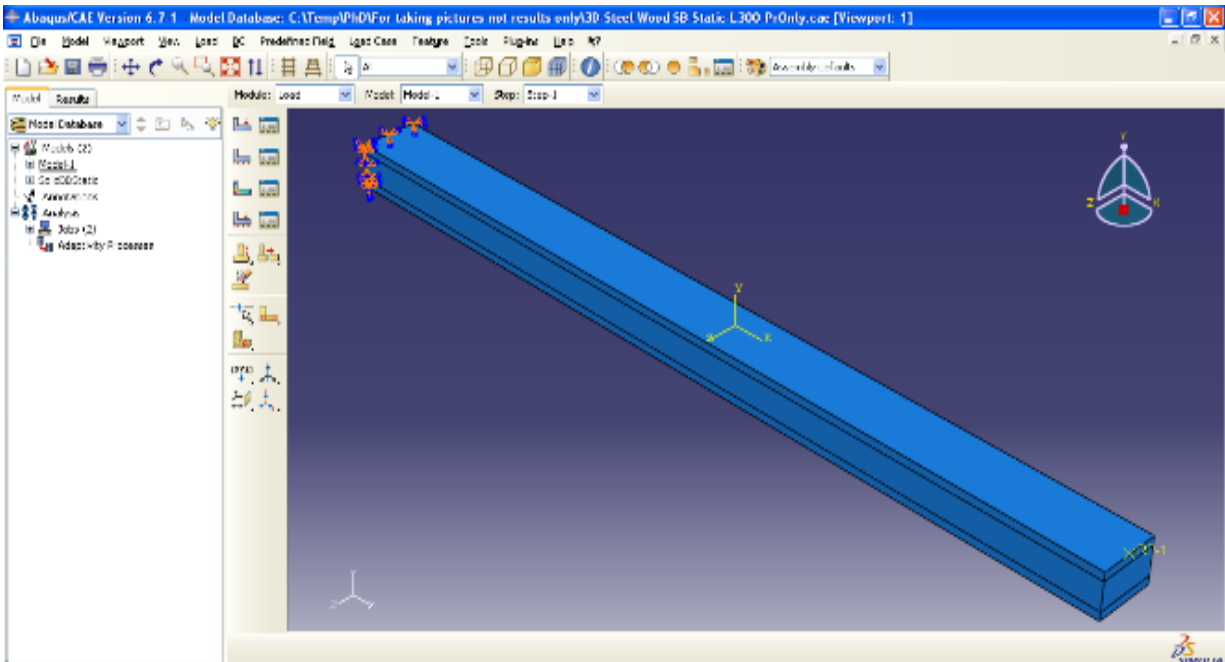


Fig. 4: Sandwich beam demonstrated as a cantilever in Abaqus software before applying a load

$$m = m_f + m_c = (\rho_f * B * L * 2h_f) + (\rho_c * B * L * h_c) \quad (8)$$

$$= BL * (2\rho_f h_f + \rho_c h_c)$$

SIMULATION ANALYSIS

Within the commercial software Abaqus 6.7-1 as shown in Fig. 4, the various sandwich beam specimens are fixed as a cantilever geometry as a constant parameter for all the demonstrated cases in this research. The main objective is obtaining numerical outputs and simulation figures for various stresses of solid and sandwich beams under different types of loads. With taking into consideration, these outputs and figures to be comparable with the theoretical results to make validation comparison.

The mechanical properties of elements of the solid beam and sandwich beams with different core material utilized in this research can be summarized in Table 1 from Abdel-Salam and Bondok (2008), beside Callister (2007).

Bending stress: A bending moment M equals 450 N.m applied perpendicular to the axis of symmetry cross-section of cantilever sandwich beam on its free end. Therefore the resultant bent sandwich beam from the Abaqus program was demonstrated in Fig. 5. While the bending strain, bending stress and specific bending stress for a core zone were illustrated through Fig. 6 to 8 respectively.

From Fig. 6, the maximum values of bending strain for the different specimens can be obtained from the outer surface of the lower face and then summarized in Table 2.

Figure 7 shows the general difference in the shape (straight and broken lines) of bending stress between a solid beam and sandwich beam. On the other hand, Fig. 8 shows the difference of bending stress for the specific core zone of three sandwich beams with a contrastive core material.

From Fig. 5 which displayed as a presentation for SB-P specimen and from Fig. 7, the maximum values of bending stress for the different specimens can be obtained from the outer surface of the lower face and then can be summarized in Table 3.

Table 1: Mechanical properties of solid beam and sandwich beam elements

Elements	Solid beam	Core		
	and face sheets	Wood	Epoxy	Polyamide
Material	Steel 1020	Wood	Epoxy	Polyamide
Modulus of elasticity (E), (GPa)	210	15	10	5.5
Density (ρ), (kg/m ³)	7900	720	1400	1300

Table 2: Maximum bending strain values at thickness -8 mm on the lower face

Specimen	SB-P	SB-E	SB-W	B-S
Bending strain (ϵ) (*10 ⁻²), (-)	0.327457	0.327182	0.326969	0.23857

Table 3: Maximum bending stress values at thickness -8 mm on the lower face

Specimen	SB-P	SB-E	SB-W	B-S
Bending stress (σ), (MPa)	698.716	691.512	687.246	514.818

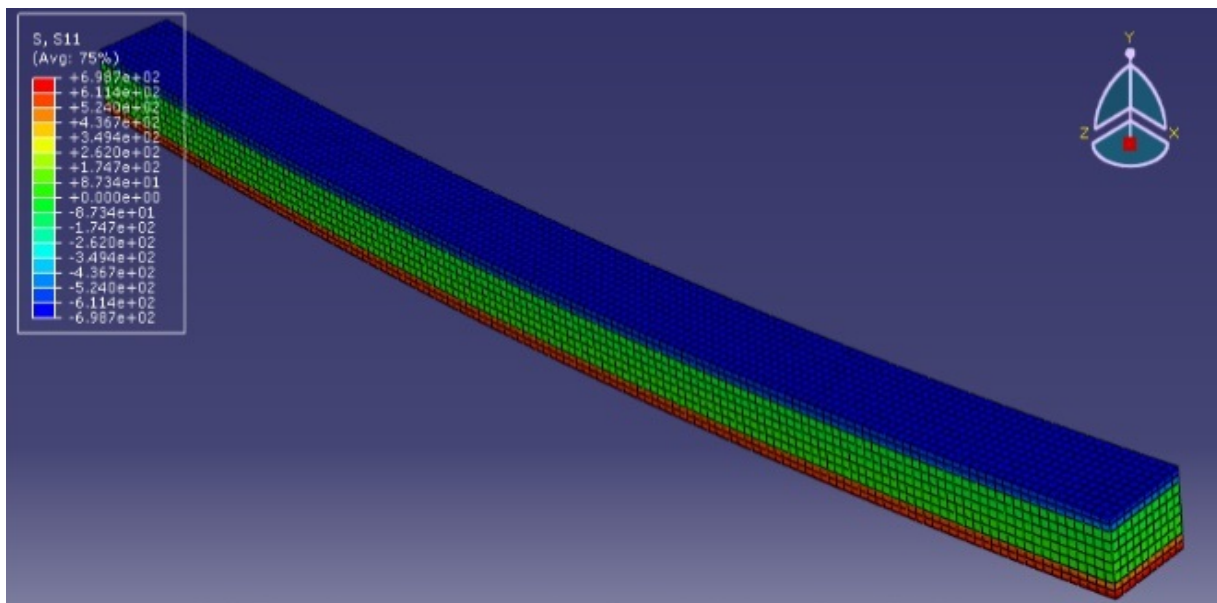


Fig. 5: Bended (SB-P) specimen after applying a moment of 450 N.m

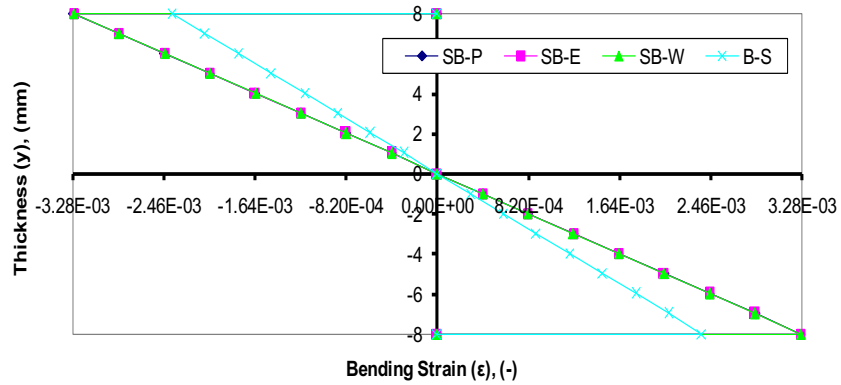


Fig. 6: Bending strain of beam versus three sandwich beams with a different core material

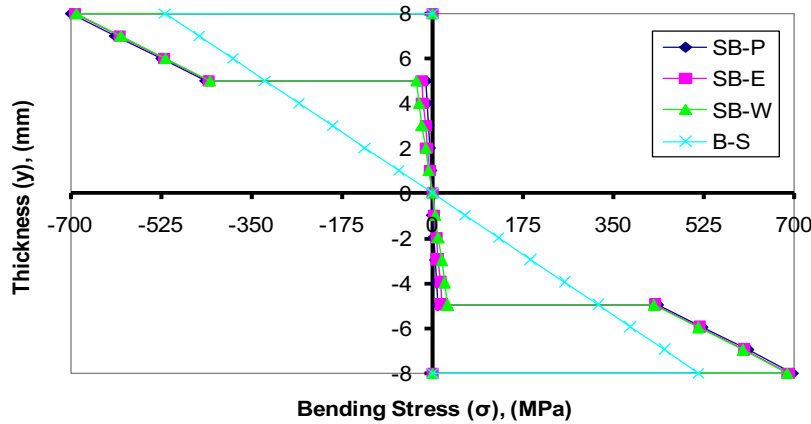


Fig. 7: Bending stress of beam versus three sandwich beams with a different core material (straight and zig-zag lines)

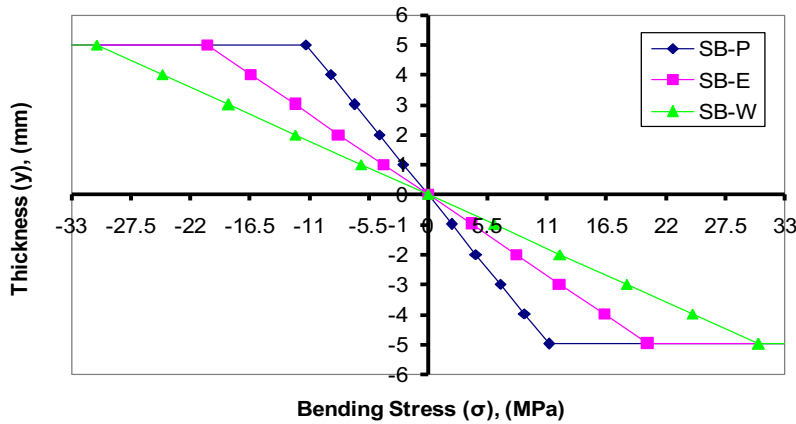


Fig. 8: Specific bending stress for the core zone of three sandwich beams with a different core material

Axial load stress: An axial load N equals 15 kN applied along the centroidal axis of cantilever sandwich beam on its free end. Therefore the resultant extended sandwich beam from the Abaqus program was demonstrated in Fig. 9. While the normal strain, normal stress and force-extension relationship were illustrated through Fig. 10 to 12 respectively.

From Fig. 10 at any thickness, the constant values of normal strain for the different axially loaded

specimens can be obtained and then summarized in Table 4.

Figure 11 shows the general C-shape of the normal stress of a sandwich beam and the natural shape of a solid beam's normal stress caused by the same axial load. On the other hand, Fig. 12 shows the various values of a force-extension relationship between solid and sandwich beams generally and especially between sandwich beams with a contrastive core material.

Table 4: Constant normal strain values at any thickness on an axially loaded specimen

Specimen	SB-P	SB-E	SB-W	B-S
Normal Strain (ϵ) ($\times 10^{-3}$), (-)	0.570343	0.551472	0.531914	0.223214

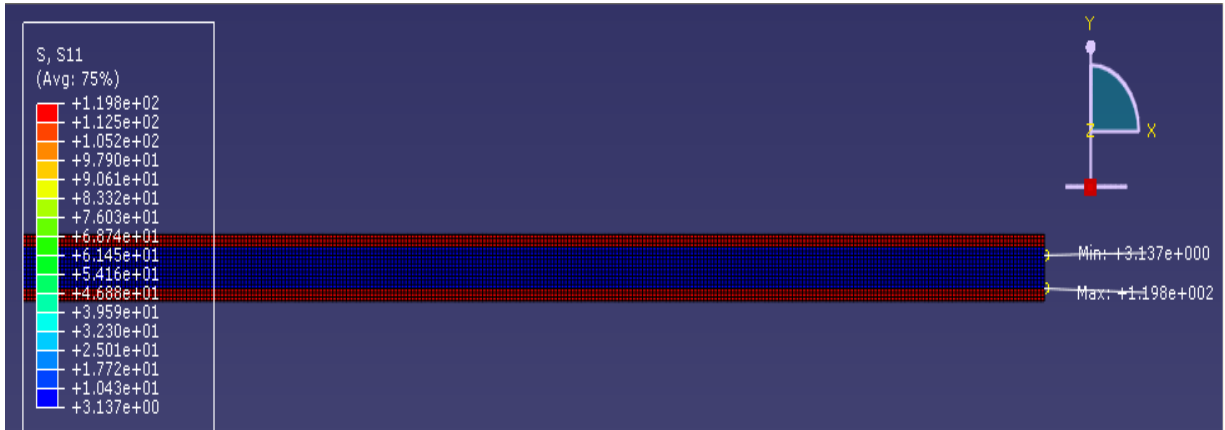


Fig. 9: Extended (SB-P) specimen after applying an axial load of 15 kN

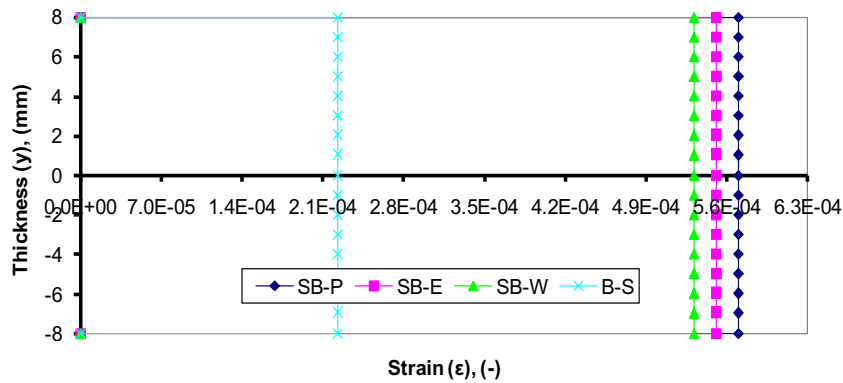


Fig. 10: Normal strain of beam versus three sandwich beams with different core material for the axially loaded case

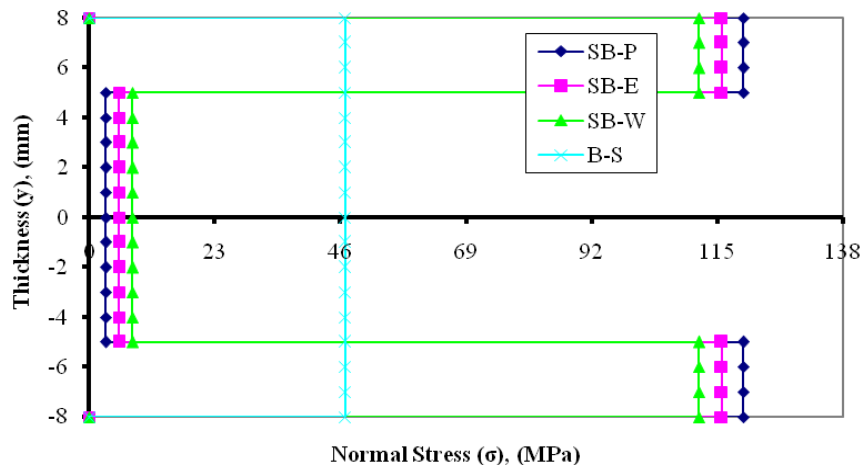


Fig. 11: Normal stress of beam versus three sandwich beams with different core material for the axially loaded case

From Fig. 11 due to axial load, the constant values of normal stress of the face sheets and the core for different sandwich beams can be obtained from any point on them; also the constant normal stress of solid

beam can be obtained and all summarized in Table 5. Beside from Fig. 12, the values of overall extension as an outcome for the axial load can be collected and summarized in Table 5.

Table 5: Constant normal stress at faces, core and solid beam, besides the extension values

Specimen	SB-P	SB-E	SB-W	B-S
Face normal stress (σ), (MPa)	119.772	115.809	111.702	46.875
Core normal stress (σ), (MPa)	3.13688	5.51472	7.97872	
Extension (ΔL), (mm)	0.171061	0.165441	0.159574	0.066964

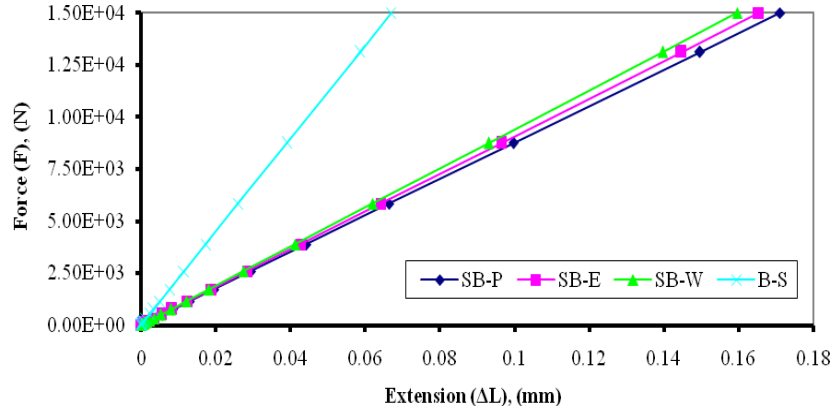


Fig. 12: Force-extension relationship of beam versus three sandwich beams with a different core material

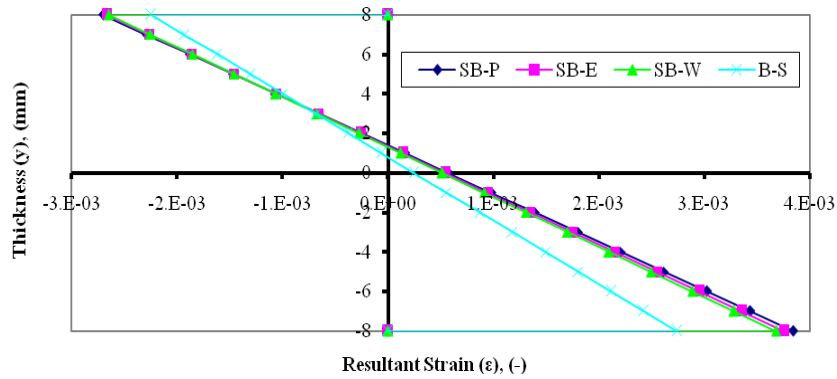


Fig. 13: A resultant strain of beam versus three sandwich beams with different core material under combined loadings

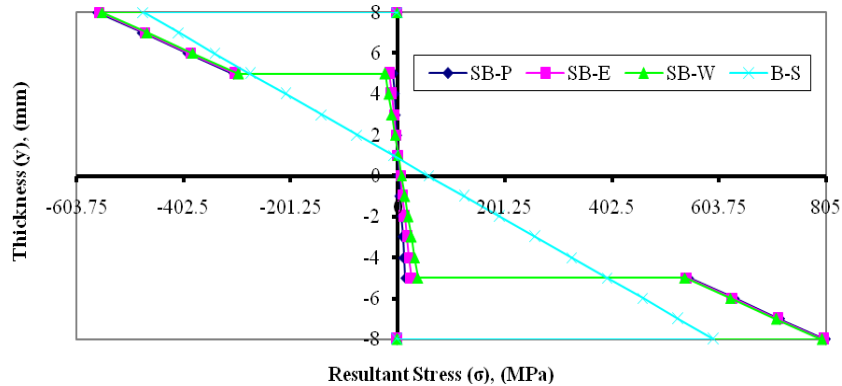


Fig. 14: Resultant stress of beam versus three sandwich beams with different core material under combined loadings

Combined loadings (axial load and bending moment): An axial load N equals 15 kN and a bending moment M equals 450 N.m, are applied simultaneously and respectively along the centroidal axis and perpendicular to the axis of symmetry cross-section of

cantilever sandwich beam on its free end. Therefore the outcomes from the Abaqus program as the resultant strain, resultant stress and specific resultant stress for a core zone were illustrated through Fig. 13 to 15 respectively.

Table 6: Maximum resultant strain of combined loadings at tension and compression sides at thicknesses -8 mm and 8 mm respectively

Specimen	SB-P	SB-E	SB-W	B-S
Tension resultant strain (ϵ) ($\times 10^{-2}$), (-)	0.384163	0.375178	0.367502	0.273857
Compression resultant strain* (ϵ) ($\times 10^{-2}$), (-)	-0.270093	-0.267007	-0.264830	-0.224646

* Compression sign (-) at specimen's upper half due to applied moment M as shown in Fig. 2 and 5

Table 7: Maximum resultant stress of combined loadings at tension and compression sides at thicknesses -8 mm and 8 mm respectively

Specimen	SB-P	SB-E	SB-W	B-S
Tension resultant stress (σ), (MPa)	804.281	800.96	797.35	595.126
Compression resultant stress (σ), (MPa)	-564.735	-560.714	-556.144	-477.828

* Compression sign (-) at specimen's upper half due to applied moment M as shown in Fig. 2 and 5

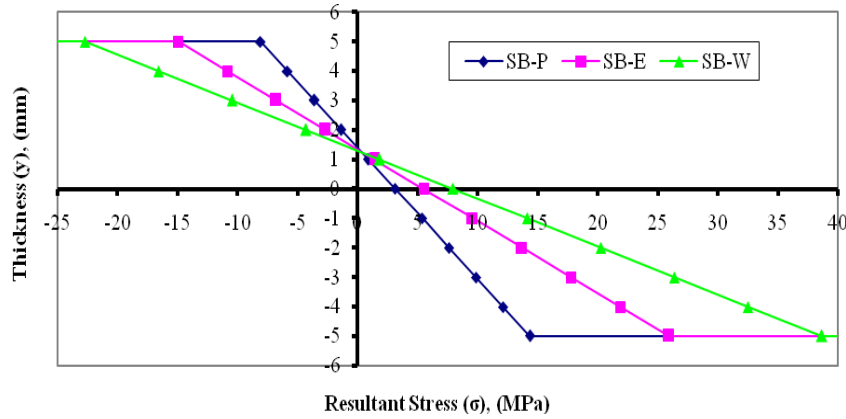


Fig. 15: Specific resultant stress for core zone of three sandwich beams with a different core material

From Fig. 13, the maximum values of resultant strain due to combined loadings for the different specimens at both tension and compression sides can be obtained from the outer surface of a lower face and upper face respectively. And then these maximum resultant strains summarized in Table 6.

Figure 14 shows the general difference in the shape of resultant stress between a solid beam and sandwich beam due to the combined axial load and bending moment, where the resultant stress distribution is linear but not passing through the point of zero stress. On the other hand, Fig. 15 shows the difference of resultant stress for the specific core zone of three sandwich beams with a contrastive core material.

From Fig. 14, as always as the resultant strain, the maximum values of resultant stress due to recently combined loadings for the different specimens at both tension and compression sides can be obtained as mentioned in Table 7.

RESULTS AND DISCUSSION

First, to validate the current theoretical and simulation results with each other, comparisons have been executed and displayed in bending study, axial load study and combined loadings (axial load and bending moment) study. Second, for the correlation and validation between the current results and results published in Ai and Weaver (2017), Kahya and Turan (2017) and Dai and Zhang (2008) besides other

researches, comparisons of methodologies have been carried out and demonstrated through Fig. 16 to 18.

Despite both current and aforesaid published results put together from studies investigate the same methodologies of bending and axial load stresses, there are general differences as the operative loads and dimensions of samples, should be taken into consideration to accept the very reasonable comparison between results.

As displayed in Fig. 16, the general C-shape of normal axial stress of a sandwich structure, which has two constant values of stresses of core and face sheets, is demonstrated in a good matching pattern in both Fig. 16(a) and (b), which leads to exhibit good support.

As shown in Fig. 17 and 18, the overall broken-line shape of bending stress of a sandwich structure, which assembled from an aggregation of bending stresses of both core and face sheets together, is demonstrated in a good matching pattern in both Fig. 17a and 17b, which leads to exhibit good support.

As displayed in Fig. 18, a good concept correlate between current results, Dai and Zhang (2008) presentation of the classic beam, homogenization and finite element methods and Kapuria *et al.* (2004) proposal of an effective zigzag one-dimensional theory of laminated beams from the point of view of the broken line theory (zig-zag theory).

Bending study: The effect of using cantilever sandwich beam instead of a solid one, on the stress analysis of applied bending moment about an axis

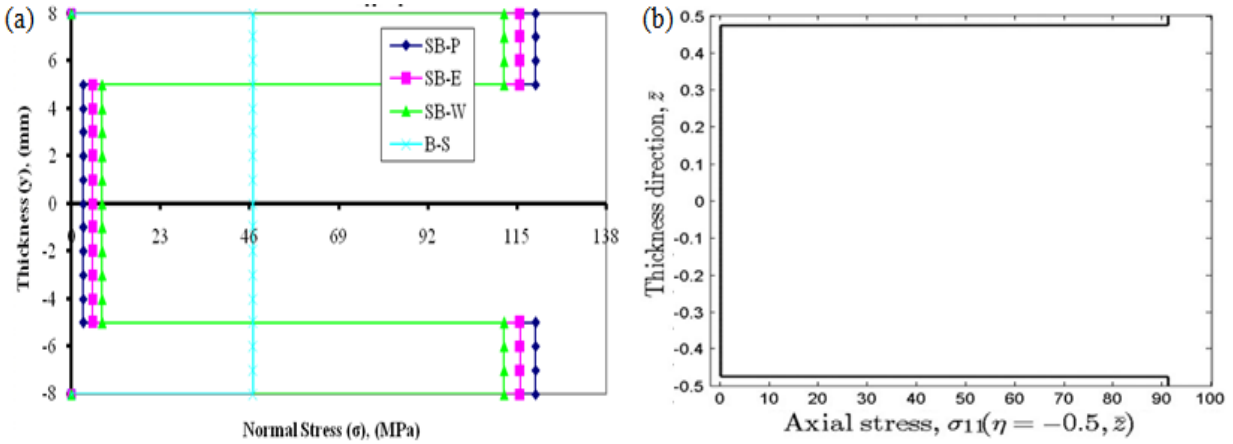


Fig. 16: Normal stress distribution of axially loaded sandwich beam: (a) from present work and (b) from Ai and Weaver (2017)

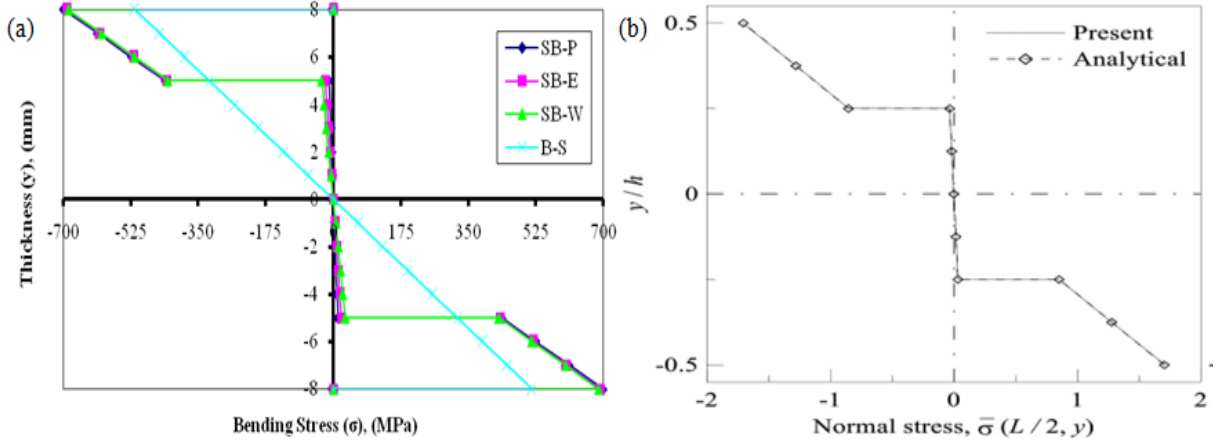


Fig. 17: Bending stress distribution of sandwich beam: (a) from present work and (b) from Kahya and Turan (2017)

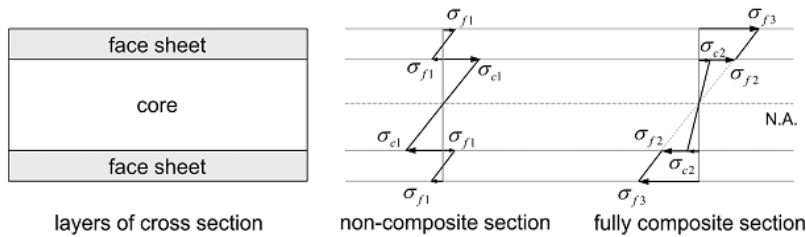


Fig. 18: Comparison of stress distribution between non-composite and fully composite sections of a sandwich panel, presented by PCI Sandwich Wall Committee (1997)

Table 8: Comparison between theoretical and simulation results of bending study at face's outer surface

Specimen	Flexural rigidity D ($\ast 10^3$), Pa.m ⁴		Bending stress σ , MPa		Bending strain ϵ ($\ast 10^{-3}$), -	
	Theoretical	Simulation	Simulation	Theoretical	Simulation	Theoretical
SB-P (n = 0.026)	1.0928	1.082	691.82	698.72	3.2944	3.2746
SB-E (n = 0.048)	1.1003	1.0933	687.11	691.51	3.2719	3.2718
SB-W (n = 0.071)	1.1086	1.1000	681.94	687.25	3.2473	3.2697
B-S (n = 1)	1.4336	1.4685	527.34	514.82	2.5112	2.3857

perpendicular to the specimen's axis of symmetry cross-section, is discussed through a presentation of

transformation factor, flexural rigidity, bending stress and bending strain in Table 8, Fig. 19 and 20.

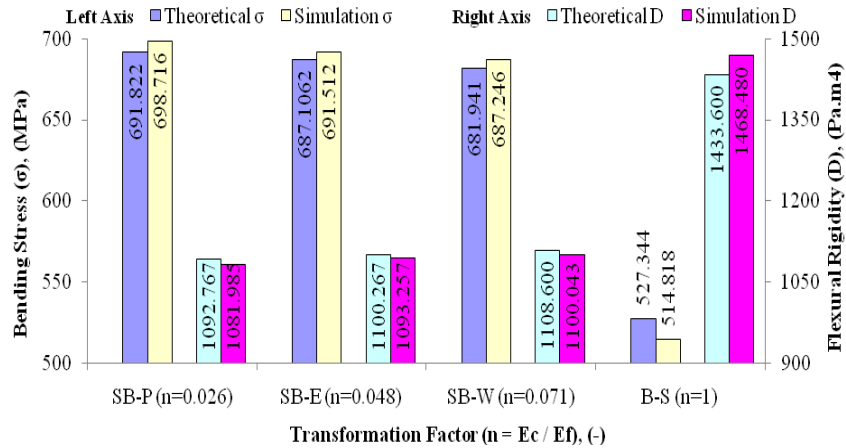


Fig. 19: Effect of sandwich beams with different core material versus solid beam on maximum bending results at face's outer surface

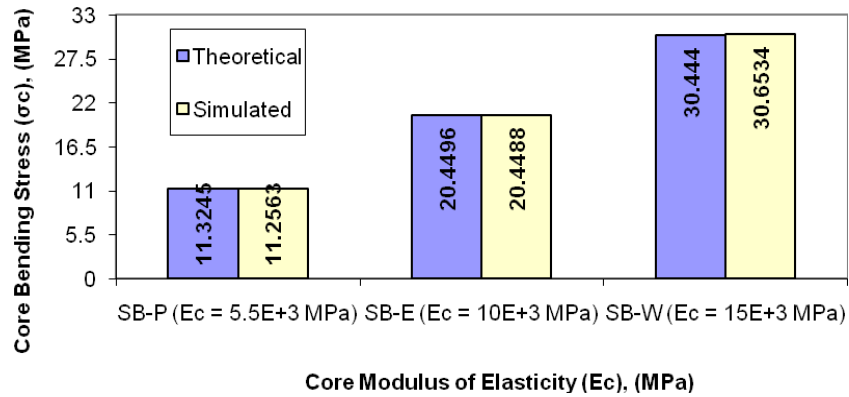


Fig. 20: Effect of core material on core bending stress at the interface between the core and face sheet

The results of bending study in comparison Fig. 19 and Table 8 exhibit good agreement by about (95%) between theoretical and simulated outcomes. As a result, using a sandwich beam with the lowest core modulus of elasticity instead of a solid beam; moderately increases the faces bending stress and strain, due to lower flexural rigidity D of the sandwich beam compared to a solid beam made from one material.

The results of core bending stress in Fig. 20 exhibit excellent agreement between theoretical and simulated outcomes. As expected, using core material with the lowest modulus of elasticity leads to a significant decrease of core bending stress due to the incremental relationship between them (E_c and σ_{Bc}) as proved in Eq. (6). With attention, this is the opposite behavior to the face bending stress as discussed in Fig. 19.

Axial load study: The effect of using cantilever sandwich beam instead of a solid one, on the stress analysis of an axial load applied along the centroidal axis of the specimen, is discussed through a presentation of transformation factor, flexural rigidity,

normal stress and normal strain in Table 9, Fig. 21 to 23.

The results of axial load study in comparison Fig. 21 and Table 9 exhibit good agreement by about (97.5%) between theoretical and simulated outcomes. As a result, using a sandwich beam with the lowest core modulus of elasticity instead of a solid beam; significantly increases the faces normal stress and strain, due to smaller transformation factor n of the sandwich beam compared to a unity one for the solid beam, as mentioned in Eq. (7).

The results of normal stress of core due to axial load in Fig. 22 exhibit excellent agreement between theoretical and simulated outcomes. As expected, using core material with the lowest modulus of elasticity leads to a significant decrease of core's normal stress, due to the decrease of the transformation factor n as mentioned in Eq. (7). With attention, that the transformation factor has the opposite effect on the face's normal stress as discussed in Fig. 21.

The results of extension caused via an axial load in Fig. 23 exhibit excellent agreement between theoretical and simulated outcomes. Authors analysis using a

Table 9: Comparison between theoretical and simulation results of axial load study at any point on the faces

Specimen	Flexural rigidity D (*10 ³), Pa.m ⁴		Normal stress σ , MPa		Normal strain ϵ (*10 ⁻⁴), -	
	Theoretical	Simulation	Theoretical	Simulation	Theoretical	Simulation
SB-P (n = 0.026)	1.0928	1.082	119.7729	119.772	5.70347	5.70343
SB-E (n = 0.048)	1.1003	1.0933	115.8088	115.809	5.5147	5.51472
SB-W (n = 0.071)	1.1086	1.1000	111.702	111.702	5.319143	5.31914
B-S (n = 1)	1.4336	1.4685	46.875	46.875	2.232143	2.23214

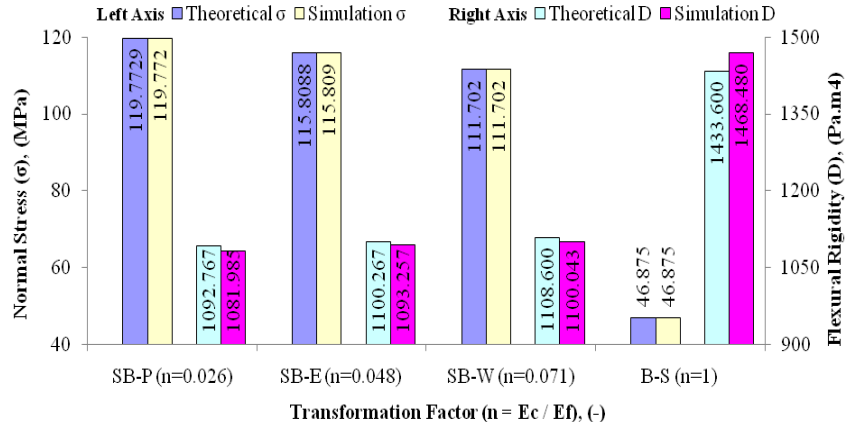


Fig. 21: Effect of sandwich beams with different core material versus solid beam on maximum axial load results at the faces

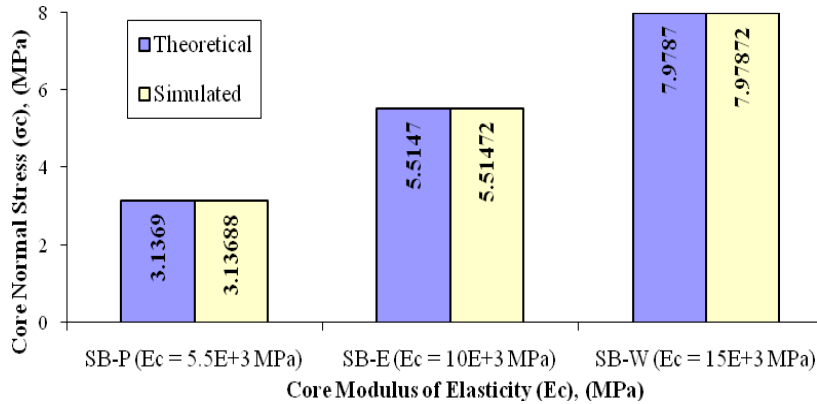


Fig. 22: Effect of core material on normal stress of core at any point on it

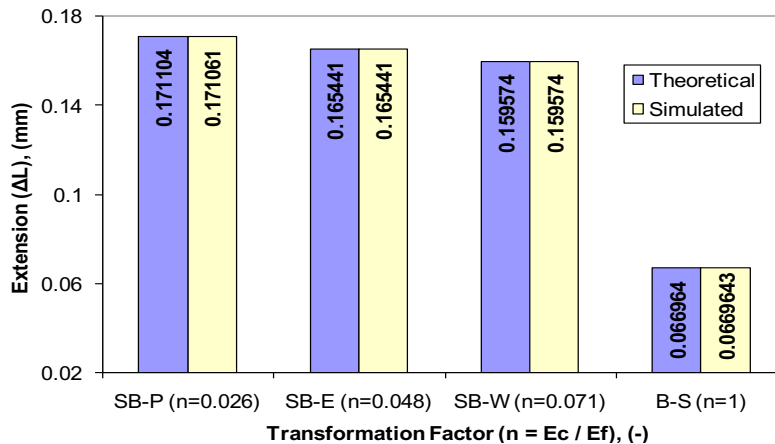


Fig. 23: Effect of specimen transformation factor on the extension

Table 10: Comparison between theoretical and simulation results of combined loadings study consists of axial load and bending moment at face's outer surface

Specimen	Flexural rigidity D ($\times 10^3$), Pa.m ⁴		Resultant stress σ , MPa		Resultant Strain ϵ ($\times 10^{-3}$), -	
	Theoretical	Simulation	Theoretical	Simulation	Theoretical	Simulation
SB-P (n = 0.026)	1.0928	1.082	811.6	804.28	3.8647	3.8416
SB-E (n = 0.048)	1.1003	1.0933	802.92	800.96	3.8234	3.7518
SB-W (n = 0.071)	1.1086	1.1000	793.65	797.35	3.7793	3.6750
B-S (n = 1)	1.4336	1.4685	574.22	595.13	2.7344	2.7386

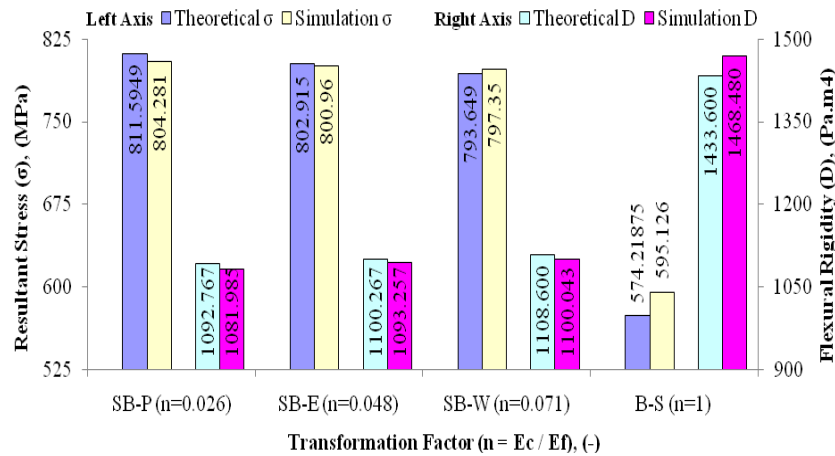


Fig. 24: Effect of sandwich beams with different core material versus solid beam on maximum results of combined axial load and bending moment at face's outer surface

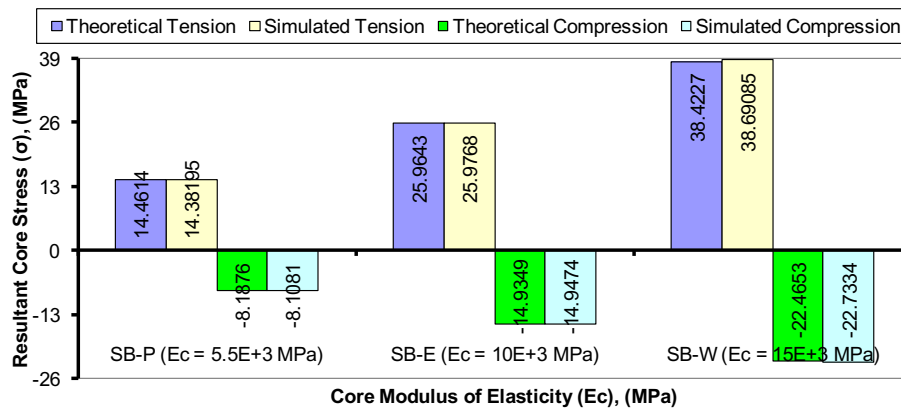


Fig. 25: Effect of core material on resultant stress of core at maximum tension and compression sides

sandwich beam with the lowest core modulus of elasticity instead of a solid beam or sandwich beam with the highest core modulus of elasticity. Therefore as expected it leads to the decrease of transformation factor n , then the increase of normal strain ϵ ; and hence significant extension increase between a sandwich beam and solid beam and slightly extension increase between different sandwich beams, as mentioned in Eq. (7).

Combined loadings (axial load and bending moment) study: The effect of using cantilever sandwich beam instead of a solid one, on the stress analysis of an axial load and a bending moment applied simultaneously on the specimen's cross-section, is

discussed through a presentation of transformation factor, flexural rigidity, resultant stress and resultant strain in Table 10, Fig. 24 and 25.

The results of combined loadings in comparison Fig. 24 and Table 10 exhibit good agreement by about (96%) between theoretical and simulated outcomes. As a result, using a sandwich beam with the lowest core modulus of elasticity instead of a solid beam; moderately increases the faces resultant stress and strain at both tension and compression sides, due to lower flexural rigidity D and lower transformation factor n of sandwich beam compared to a solid beam.

The results of core's resultant stress of in Fig. 25 exhibits excellent agreement between theoretical and

simulated outcomes. As expected, using core material with the lowest modulus of elasticity leads to significant decrease of core's resultant stress at both tension and compression sides, due to the incremental relationship between them (E_c , σ_{Bc} and σ_{Nc}) as proved in Eq. (6) and Eq. (7). With attention, this is the opposite behavior to the face's resultant stress as discussed in Fig. 24.

CONCLUSION

Authors present results of the current research based on utilization the main advantage of a sandwich beam, which is high strength and stiffness to weight ratio and where loadings applied on the free end of a cantilever geometry. Therefore, from using steel polyamide Sandwich Beam (SB-P) with low core modulus of elasticity instead of a solid steel beam (B-S) having the same dimensions, in other words, via significantly decreasing the transformation factor by about 97%, also means moderately decreasing the flexural rigidity by about 24% and finally means moderately decreasing the weight by about 50%; it can be concluded that:

The faces bending stress and strain are moderately increasing by about 35% and vice versa.

In the case of axial load the extension, faces normal stress and strain are significantly increased by about 150% and vice versa.

In case of combined loadings contain axial load and bending moment, the faces resultant stress and strain at tension side are moderately increasing by about 40%, while at compression side they are moderately increasing by about 20% and vice versa.

Also authors study the effect of changing core material via utilization (SB-P) with lower core modulus of elasticity than a steel wood sandwich beam (SB-W), in other words, via significantly decreasing the transformation factor by about 63%, also means slightly decreasing the flexural rigidity by about 1.4% and finally means slightly decreasing the weight by about 10%; therefore it can be concluded that:

As opposite behavior to the face bending stress, the core bending stress is significantly decreasing by about 63% and vice versa.

Here, the overall extension caused by an axial load is slightly increased by about 7% and vice versa. As opposite behavior to the face's normal stress, the core's normal stress is significantly decreasing by about 60% and vice versa.

As opposite behavior to the face resultant stresses caused by an axial load and a bending moment, the core's resultant stresses at both tension and compression sides are significantly decreasing by about 62% and vice versa.

The obtained results theoretically and simulation were compared with each other, which indicate a close

agreement between them by about 95%. Therefore the theoretical and simulation analysis can be used in the design stage to select the best from the different sandwich beam variables and configurations to increase its advantages which make it attractive for varied applications, where high stiffness to weight ratio, flexibility and carrying loads are required.

Nomenclature:

A	: Cross-sectional area of the sandwich beam (m^2)
B	: Width of the sandwich beam (m)
c	: Neutral line offset (m)
D	: Flexural rigidity or bending stiffness ($Pa.m^4$)
D_{co}	: Flexural rigidity of a core about its own neutral line and also about the neutral line of the entire sandwich beam ($Pa.m^4$)
D_f	: Flexural rigidity of each face sheet about its own neutral line ($Pa.m^4$)
D_{fn}	: Flexural rigidity of the face sheets about the neutral line of the entire sandwich beam ($Pa.m^4$)
d	: Distance between the neutral lines of symmetric top and bottom layers (m)
E_1, E_3, E_f	: Modulus of elasticity of the face sheet (GPa)
E_c	: Modulus of elasticity of the core (GPa)
E_{eq}	: Equivalent modulus of elasticity of the entire sandwich beam (GPa)
E_i	: Modulus of elasticity of a specific layer (GPa)
F	: Force (N)
H	: Total thickness of the sandwich beam (m)
h_1, h_3, h_f	: Thickness of the face sheet (m)
h_2, h_c	: Thickness of the core (m)
I	: Area moment of inertia of the sandwich beam (m^4)
L	: Length of the sandwich beam (m)
L_o	: Original length of the sandwich beam (m)
ΔL	: Change in length or extension (m)
M, M_b	: Bending moment (N.m)
m	: Total mass of the sandwich beam (kg)
m_c	: Mass of the core (kg)
m_f	: Mass of the face sheets (kg)
N	: Axial load (kN)
n	: Transformation factor as a ratio between core and face sheet moduli of elasticity (-)
R	: Radius of curvature (m)
x, z	: Coordinates (m)
y, y_0, y_1, y_2, y_3	: Coordinates in the thickness direction of a sandwich beam (m)
ε	: Strain (-)

ϵ_{Bc}	: Bending strain of a core material (-)
ϵ_{Bf}	: Bending strain of a face sheet (-)
ϵ_{Nc}	: Normal strain of a core material due to axial load (-)
ϵ_{Nf}	: Normal strain of a face sheet due to axial load (-)
ρ	: Density of a material (kg/m ³)
ρ_c	: Density of the core material (kg/m ³)
ρ_f	: Density of the face sheets material (kg/m ³)
σ	: Stress (MPa)
σ_{Bc}	: Bending stress of a core material (MPa)
σ_{Bf}	: Bending stress of a face sheet (MPa)
σ_{Nc}	: Normal stress of a core material due to axial load (MPa)
σ_{Nf}	: Normal stress of a face sheet due to axial load (MPa)
(B-S)	: Solid beam of a steel material
(SB-E)	: Sandwich beam of steel epoxy
(SB-P)	: Sandwich beam of steel polyamide
(SB-W)	: Sandwich beam of steel wood

REFERENCES

- Abdel-Salam, M. and N.E. Bondok, 2008. Theoretical and experimental investigations into the effect of the sandwich beam elements on its dynamic characteristics. *Ain Shams J. Mech. Eng.*, 2: 91-110.
- Ai, Q. and P.M. Weaver, 2017. Simplified analytical model for tapered sandwich beams using variable stiffness materials. *J. Sandwich Struct. Mater.*, 19(1): 3-25.
- Ashby, M.F., A.G. Evans, N.A. Fleck, L.J. Gibson, J.W. Hutchinson and H.N.G. Wadley, 2000. *Metal Foams: A Design Guide*. 1st Edn., Butterworth-Heinemann, Oxford.
- Banerjee, J.R., C.W. Cheung, R. Morishima, M. Perera and J. Njuguna, 2007. Free vibration of a three-layered sandwich beam using the dynamic stiffness method and experiment. *Int. J. Solids Struct.*, 44(22-23): 7543-7563.
- Barbieri, L., R. Massabò and C. Berggreen, 2018. The effects of shear and near tip deformations on interface fracture of symmetric sandwich beams. *Eng. Fract. Mech.*, 201: 298-321.
- Bozhevolnaya, E., A. Lyckegaard and O.T. Thomsen, 2008. Novel design of foam core junctions in sandwich panels. *Compos. Part B-Eng.*, 39: 185-190.
- Callister, W.D., 2007. *Materials Science and Engineering: An Introduction*. 7th Edn., John Wiley and Sons, Inc., New York.
- Chen, C., A.M. Harte and N.A. Fleck, 2001. The plastic collapse of sandwich beams with a metallic foam core. *Int. J. Mech. Sci.*, 43(6): 1483-1506.
- Dai, G.M. and W.H. Zhang, 2008. Size effects of basic cell in static analysis of sandwich beams. *Int. J. Solids Struct.*, 45(9): 2512-2533.
- Ferdous, W., A. Manalo, T. Aravinthan and A. Fam, 2018. Flexural and shear behaviour of layered sandwich beams. *Constr. Build. Mater.*, 173: 429-442.
- Fleck, N.A. and V.S. Deshpande, 2004. The resistance of clamped sandwich beams to shock loading. *J. Appl. Mech.*, 71(3): 386-401.
- Gibson, L.J. and M.F. Ashby, 1997. *Cellular Solids: Structure and Properties*. 2nd Edn., Cambridge University Press, Cambridge.
- Jen, Y.M. and L.Y. Chang, 2009. Effect of thickness of face sheet on the bending fatigue strength of aluminum honeycomb sandwich beams. *Eng. Failure Anal.*, 16(4): 1282-1293.
- Kahya, V. and M. Turan, 2017. Bending of laminated composite beams by a multi-Layer finite element based on a higher-order theory. *Acta Phys. Polonica A*, 132: 473-475.
- Kapurja, S., P.C. Dumir and N.K. Jain, 2004. Assessment of zigzag theory for static loading, buckling, free and forced response of composite and sandwich beams. *Composite Struct.*, 64(3-4): 317-327.
- Kim, J. and S.R. Sawnson, 2001. Design of sandwich structures for concentrated load. *Composite Struct.*, 52(3-4): 365-373.
- Lu, G. and T.X. Yu, 2003. *Energy absorption of structures and materials*. 1st Edn., Woodhead Publishing Ltd., Cambridge.
- Magnucka-Blandzi, E. and K. Magnucki, 2007. Effective design of a sandwich beam with a metal foam core. *Thin-Walled Struct.*, 45(4): 432-438.
- McCracken, A. and P. Sadeghian, 2018a. Corrugated cardboard core sandwich beams with bio-based flax fiber composite skins. *J. Build. Eng.*, 20: 114-121.
- McCracken, A. and P. Sadeghian, 2018b. Partial-composite behavior of sandwich beams composed of fiberglass facesheets and woven fabric core. *Thin-Walled Struct.*, 131: 805-815.
- McShane, G.J., V.S. Deshpande and N.A. Fleck, 2007. The underwater blast resistance of metallic sandwich beams with prismatic lattice cores. *J. Appl. Mech.*, 74(2): 352-364.
- PCI Sandwich Wall Committee, 1997. State-of-the-art of pre-cast/prestressed sandwich wall panels. *J. Pre-cast/Prestressed Concrete Institute*, 42(2): 1-60.
- Romanoff, J., P. Varsta and A. Klanac, 2007. Stress analysis of homogenized web-core sandwich beams. *Compos. Struct.*, 79(3): 411-422.
- Steeves, C.A. and N.A. Fleck, 2004. Material selection in sandwich beam construction. *Scripta Mater.*, 50(10): 1335-1339.
- Xue, Z. and J.W. Hutchinson, 2004. A comparative study of impulse-resistant metal sandwich plates. *Int. J. Impact Eng.*, 30(10): 1283-1305.